Proceedings of the Canadian Society for Mechanical Engineering International Congress
32nd Annual Conference of the Computational Fluid Dynamics Society of Canada
Canadian Society of Rheology Symposium
CSME-CFDSC-CSR 2025
May 25–28, 2025, Montréal, Québec, Canada

ANALYSIS OF TOPOGRAPHY FORMATION DURING SURFACE STRUCTURING BY LASER REMELTING

Ekaterina Akopyan[1], Evgueni V. Bordatchev[2,1*], O. Remus Tutunea-Fatan[1,2**]
[1]Department of Mechanical and Material Engineering, Western University, London, Canada
[2]Automotive and Surface Transportation, National Research Council of Canada, London, Canada
[*]evgueni.bordatchev@nrc-cnrc.gc.ca, [**]rtutunea@eng.uwo.ca

Abstract **–** Surface topographies with specific geometric structures enable functionalities such as friction control, optical tuning, and aerodynamic optimization. Laser-based techniques such as direct laser writing and interference patterning create functional surfaces at micro- and nanoscales but rely on material removal. By contrast, laser remelting (LRM) redistributes molten material without adding or removing it, thus offering a novel approach to surface structuring. This study investigates LRM for fabricating sine-structured surfaces (SSS) subjected to a 15 W ± 5 W laser power modulation and scanning speeds of 100–500 mm/s. Form non-uniformity parameters – including period, amplitude, and phase shift - were analyzed and revealed that the scanning speed significantly affects structure formation. While 100, 200, 400, and 500 mm/s produced stable structures, 300 mm/s resulted in the highest deviations, suggesting instability. These findings highlight the importance of LRM process parameters in achieving consistent structures. Future research will focus on real-time thermographic monitoring to better understand LRM thermodynamics and explore its applications in aerospace, automotive, marine, energy, and biomedical sectors.

Keywords-surface structuring; laser remelting; topography; formation; analysis

I. INTRODUCTION

The constant evolution of modern engineering and technology drives the need for advancements in manufacturing processes, particularly with respect to productivity and accuracy. Along these lines, one of the relatively new research areas focuses on functional surfaces that essentially rely on modifications brought to surface topography to improve their performance for various applications. Nonetheless, advanced micromanufacturing technologies are needed to generate complex functional geometries. Present microfabrication techniques include material removal procedures such as cutting, laser ablation, and electron beam.

Laser ablation involves the use of laser beam radiation to heat workpiece material until evaporation in order to precisely remove it and thereby alter surface topography as desired. Laser ablation typically encompasses three processes: direct laser writing, laser induced surface structuring, and direct laser interference patterning [1]. Unlike the conventional surface topography modification (STM) process that involves material removal, an innovative method has been developed to reallocate material in its molten state under the influence of a high-energy source, such as an electron or laser beam. Along these lines, it was shown [2] that micro-bumps can be formed on a glass surface by changing the state of the thermodynamic equilibrium during the rapid heating-cooling cycle controlled by a CO_2 laser. During this cycle, the microstructural change associated with relaxation occurs and leads to density reduction and therefore volumetric expansion of approximately 2–3% in the heat affected zone. As a result, bumps with a height of up to 0.1 µm have been formed for potential applications in micro-optics. A variant of the STM process – called Surfi-Sculpt – was developed by TWI Ltd. (Cambridge, UK) [3]. Surfi-Sculpt uses electron beam energy to melt and manipulate metal surfaces into intricate structures, offering versatility for applications such as surface coatings, heat exchangers, and biomedical implants [4]. In a subsequent advancement towards the development of the STM process, electron beam energy was replaced with high-power laser radiation, enabling intensive development of the STM processes by laser remelting (LRM) for a variety of functional topographies [5-8]. Techniques like laser texturing, selective laser sintering, and electron beam processing create hierarchical structures with tailored properties. By modifying surface topography at micro and nano scales, these methods enhance material performance for applications in optics, lubrication, wear resistance, biointeraction, fatigue resistance, and composite bonding, improving strength and durability [4].

The continuous advancement in texturing and structuring technologies represents an asset towards the development of next generation materials and devices that essentially drives innovation across various industries. This includes the

This research was funded by the Natural Science Engineering Research Council of Canada under grants RGPIN/6616-2019 and RGPIN/5126-2019.

development of alternatives to current technologies, namely surface structuring by laser remelting (SS-LRM) that represents the focus of the present study. SS-LRM relies on laser energy to modify the topography of a surface without ablating the material. Unlike subtractive processes like cutting or laser ablation, where material removal is irreversible, SS-LRM allows molten material to relocate before solidifying. This reversibility makes SS-LRM a versatile and effective technique for various applications [9, 10]

STM-LRM is characterized by numerous technological advantages granted by some of its features and/or parameters such as processing speed, versatility, CNC programmability, multi-axis control, etc. One of the STM-LRM parameters is constituted by the phase shift between the control signal (laser power, speed, focus distance) and surface topography formation, has a critical importance [8-10]. This causes a deviation between programmed (desired) and actual topography profiles and therefore requires the development of advanced control strategies to compensate for these deviations online/in realtime. During the formation of sine-shaped topographies through laser power modulation, the control-to-surface phase influences deviations in profile height, structure period, and phase shift, as well as the occurrence of saddle points, asymmetry, or rounding of the structure [10].

To investigate some of these parameters, the present study will be focused on the preliminary analysis of topography formation during the STM-LRM process by means of the aforementioned parameters that are characteristic to structural nonuniformity. The study will also detail an experimental setup to be used for the generation of sine-surface structuring by laser remelting (SSS-LRM) while only varying the laser scanning speed. A methodology for the analysis of the fabricated sine-structures will be presented and key non-uniformity parameters will be analyzed in detail.

II. LRM System for SSS and Analysis Methodology

A. SSS-LRM System

The system used to perform the SSS-LRM experiments (Fig. 1) was developed at the National Research Council (NRC) laboratory (London, ON, Canada) and integrates several process-enabled opto-electro-mechanical components: 1) three-axis motion system from AEROTECH, Inc. (Pittsburg, PA, USA) mounted on a granite table for precisely positioning a workpiece within a work envelope; 2) two-axis laser scanner from SCANLAB GmbH (Puchheim, Germany) with a *f*-theta lens, having a focusing distance of 256 mm; and 3) continuous wave (cw) laser from IPG Photonics, Inc. (Oxford, MA, USA) with a wavelength of 1070 nm and power up to 100 W, delivering a laser beam via an optical fiber into the laser scanner after collimating. A Windows-based PC acted as a control unit integrating two controls software – one from AEROTECH, Inc. for CNC programming and motion control of kinematic XYZ stages, and the second one, a LaserPC software from the Fraunhofer Institute for Laser Technology (Aachen, Germany) for synchronous control of the X_s-Y_s scanner positions and laser power. A workpiece with 50 mm × 50 mm × 10 mm dimensions from ground H13 tool steel was mounted on X-Y kinematic stages within an Argon-filled enclosure to prevent oxidation.

During the SSS-LRM experiments, five surface structures with a period of 500 µm were created on the workpiece with an area of 0.8 mm × 10 mm, each filled with a stepover of 20 µm between adjusted laser tracks. To maintain consistent process conditions for each laser track, a unidirectional trajectory was applied for when the laser is turned on at the beginning and turned off at the end of each laser track. The same laser power variation of 15 W ± 5 W was applied for creating all structures while using different scanning speeds: 100 mm/s, 200 mm/s, 300 mm/s, 400 mm/s, and 500 mm/s as a logical continuation of our previous studies [8]. These process parameters were selected to examine in detail the aspects of thermodynamic flow of molten material during the SSS-LRM process.

B. Methodology of Data Analysis

As already indicated, this study focuses on the analysis of the formation of surface structures under controlled variations in laser power. The effect of scanning speed was also considered, since it influences processing time and fabrication cost while ensuring acceptable form accuracy and precision. The methodology for the analysis of the surface topography formation ($h(x,y)$) (Fig. 2), considers the two most critical aspects of the SS-LRM process: i) structured topography formation, $h_{SS}(x,y)$, wrt the initial surface topography, $h_{ini}(x,y)$, and ii) structure formation wrt commanded laser power control signal, $P(x,y)$. Each aspect of the structured surface topography formation requires the analysis of the specific areal component of $h(x,y)$.

For the analysis of $h_{SS}(x,y)$, two longitudinal profiles should be compared (Fig. 2b), namely: $h_{SS}(x_{center},y)$ taken at the center of the structured area and $h_{ini}(x_{ini},y)$, taken as close as possible to $h_{SS}(x,y)$. These three profiles are to be plotted together for a detailed analysis. However, single profile analysis may not bring all statistically reliable parameters of the surface formation (period and amplitudes), because they are very localized.

To increase the reliability of the surface topography formation, the topography of the initial surface $h_{ini}(x_{ini},y)$ had to be eliminated from the analysis. Further, the locations where laser power was turned on and off were also excluded from the analysis, since SSS-LRM is not stable at these locations. These exclusions will define surface area structured by the stationary SSS-LRM process performance, namely $h_{SSstat}(x,y)$. This area constitutes the focus of the analysis because it is unaffected by the $h_{ini}(x,y)$ and any variations in the LRM process performance. Several parameters of stationary formation of the surface sine-structures can be subsequently analyzed as follows:

- Determine all longitudinal profiles across the width ($h_{SSstat}(x_{width},y)$);
- Calculate the average longitudinal profile ($\hat{h}_{STstat}(y)$) for the entire stationary area according to: $\hat{h}_{SSstat}(y) = mean_{width}(h_{SSstat}(x_{width},y))$;
- Separate $\hat{h}_{SSTstat}(y)$ into a sequence of N individual periods: $\hat{h}_{SSstat}(y) = \sum \mathbf{T}_i$, $i = 1 \ldots N$;
- Calculate all parameters of each $\mathbf{T}_i$, such as, the period duration T_i, highest amplitude $Hhigh_i = max(\mathbf{T}_i)$, lowest amplitude $Hlow_i = min(\mathbf{T}_i)$, magnitude

$H_i = H_{high_i} - H_{low_i}$, and their mean and standard deviation (STD) values for an averaged $\overline{\mathbf{T}}_{SS}$;

- Determine the critical parameter termed as phase shift and its sign between the averaged $\overline{\mathbf{T}}_{SS}$ and the ideal period of the control function $P(x,y)$ as $\Delta T_{SS\text{-}P}(y)$.

The information above provides guidelines for conducting SSS-LRM experiments and specifies the required data collection as well as its analysis methods. This information also outlines a clear path toward the targeted objective: investigation of the effect of scanning speed on surface structure formation under power-controlled SSS-LRM conditions.

III. Analysis of Sine Surface Topography Formation

To investigate the effect of scanning speed on the formation of surface sine-structures during LRM, five experiments were conducted, each with varying laser scanning speeds (100 to 500 mm/s) while maintaining constant power settings. The primary objective was to extend our previous work [8], create 3D sinusoidal structures with a desired period of 500 µm, and to analyze the actual surface topography for deviations from the desired profile without examining surface quality (R_z, R_a, etc.)

The fabricated surface topographies and their longitudinal profiles (initial, desired, and actual middle) are presented in Fig. 3 for all five scanning speeds. The surface topographies of 10 mm (length) × 1 mm (width) areas were measured by means of an optical interferometer WYKO NT1100 (Veeco Ltd., USA) with a vertical resolution of 0.1 nm and an X-Y grid size of 192.98 nm. As a reference for the comparison with the initial surface, 1 mm space of the original surface was allocated at the edges of the SSS. Fig. 3 depicts an overall 3D view of the sine-structured surfaces (Fig. 3 left) as well as a visual 1D appearance of the transformation of the initial surface's longitudinal profile into an actual middle one with respect to the desired profile (Fig. 3 right). Both 1D and 2D SSS require individual considerations and analysis.

At the start of each SSS, a noticeably deeper initial cavity emerges. This feature is also visible in the longitudinal profiles and it can be assumed that is occurrence is a consequence of the transient behavior of the LRM at the beginning of each laser track that is in turn driven by the combined effects of acceleration as well as powering on the laser. Therefore, this region of the SSS is characterized by more laser energy delivered per unit area to the surface. The stationary regime of the SSS-LRM follows the transient one, and therefore the sine-structures produced by the stationary regime only were further used for the analysis. Furthermore, the very last period of the generated sine-structures was also excluded from the analysis because it ended up being incomplete in most situations due to the different scanning speeds. A space of 0.1 mm from the left and right sides of the sine-structured topography was excluded from the analysis since in this region structures are gradually morphing into the initial surface.

The subsequent analysis of sine-structured surfaces (Fig. 4) revealed that their longitudinal profiles were not consistent and repeatable (Fig. 4 left). This prompted the analysis of all longitudinal profiles both individually and collectively across the structured area. To address this, several additional parameters were calculated for each SSS: mean and standard deviation (STD) of periods, amplitudes, period by peaks and valleys, and phase shift between (bw) actual and desired profiles. All calculated parameters of SSS are summarized in Table 1.

The experimental findings show that changes in scanning speed affect the periodic accuracy and stability of the sin-structures. Each period exhibits three defining features: peaks, valleys, and the zero-crossing in each cycle. Because half of the amplitude lies above and half below zero, this setup permits a detailed examination of structural symmetry – or the accuracy of the periodic profile – that could be explored more extensively in future studies.

According to the data presented, mean period durations remained consistent across most speeds, slightly increasing for 495.0 µm for 100 mm/s to 496.0 µm at 500 mm/s. However, there is a noticeable decrease of the sine-structure period by 28 µm at 300 mm/s (e.g., 467.0 µm vs typical ~495.0 µm). Similarly, the standard deviation (STD) of periods (a metric of the stability of the LRM process) spiked significantly at 300 mm/s (e.g., 107.0 µm) compared to the much lower values for other speeds. This suggests that the process is least stable at 300 mm/s, with the mean of period amplitudes exhibiting a similar trend; with the lowest amplitude occurring at 300 mm/s (8.5 µm) and higher values observed at the slower and faster speeds. This deviation suggests a loss of the sine-structure formation stability at this specific speed.

TABLE I. Calculated Parameters of Sine-Structure Surfaces

Parameter (um)	Speed (mm/s)				
	100	***200***	***300***	***400***	***500***
Mean period, µm	495.0	495.0	467.0	496.0	496.0
STD of periods, µm	17.0	21.0	107.0	23.0	16.0
Mean of amplitudes, µm	13.0	10.7	8.5	11.4	13.9
STD of amplitudes, µm	0.9	1.4	2.2	1.4	1.0
Mean of peaks, µm	6.7	5.6	4.4	6.0	7.3
STD of peaks, µm	0.6	0.9	1.4	0.9	0.6
Mean of valleys, µm	-6.3	-5.1	-4.1	-5.4	-6.6
STD of valleys, µm	0.8	0.9	1.1	0.9	0.8
Mean shift bw periods, µm	0.2	0.2	0.3	0.2	0.2
Mean shift bw profiles, deg	-107.9	-129.2	-229.6	-129.0	-108.1
STD of shift bw profiles, deg	23.0	22.0	228.0	21.0	20.0

Meanwhile, the STD of period amplitude (an indicator of process variability), peaked at 300 mm/s (by 2.2 µm), once again suggesting that this speed introduces significant inconsistencies in feature height. The mean of period peaks and valleys, as well as their respective standard deviations, further demonstrate these same results. Peaks were lowest at 300 mm/s (by 4.4 µm), and valleys were shallowest (by -4.1 µm), both indicating a reduced depth of the sine-structures. The higher instability in these values, represented by their standard deviations, again peaked at 300 mm/s, thus confirming a reduced process reliability at this speed. The mean shift between periods remained small (0.2–0.3 µm) across all speeds, suggesting a minimal displacement in the periodic profile. However, the mean shift between periods showed a more significant deviation at 300 mm/s (by - 229.6 deg), as opposed to more consistent values at other speeds (-107.9°deg to -129.2°deg). This larger phase shift at 300 mm/s reflects a significant misalignment between the programmed and achieved periods, directly impacting the

accuracy of the sine-structured profiles. This insight is essential for future extensions of this research aimed at real-time control of the SSS-LRM process, in which the phase shift must be taken into account due to its direct impact on the positional accuracy.

From these observations, the 300 mm/s scanning speed represents a critical point of instability for the SSS-LRM process. At this speed, all major parameters, including period durations, amplitudes, peaks, valleys, and phase shifts, deviate significantly from their correspondents associated with other speeds whereas the higher variability (suggested by STD) indicates a reduced process reliability. By contrast, the results obtained at 100 mm/s, 200 mm/s, 400 mm/s, and 500 mm/s demonstrate better consistency and accuracy, suggesting these speeds are more suitable for producing high-quality sine-structured topographies.

IV. Summary and Conclusions

The experimental analysis demonstrates that laser scanning speed significantly affects the formation and stability of sinusoidal structures during SS-LRM processing. While scanning speeds of 100 mm/s, 200 mm/s, 400 mm/s, and 500 mm/s resulted in consistent and accurate profiles with minimal deviations from the ideal geometry, a critical instability was observed at 300 mm/s. At this speed, parameters such as period durations, amplitudes, peaks, valleys, and phase shifts exhibited notable deviations and increased variability, indicating reduced process reliability and structural accuracy. The phase shift at 300 mm/s was particularly significant, highlighting a misalignment between programmed and achieved periods, and this can impact future implementations of the process. These findings suggest that scanning speeds outside the critical instability range, particularly 100 mm/s and 200 mm/s, are optimal for achieving stable and precise surface structuring, certain speed values – such as 300 mm/s – should be avoided due to their reduced reliability and higher variability. Standard deviations were calculated for each scanning speed and maximum values were found at 300 mm/s suggesting the source of process instabilities associated with this speed.

Future research could explore varying laser intensity at a constant scanning speed to investigate additional process parameters, employing different formation intervals, and integrating real-time monitoring of the SSS-LRM process through thermographic imaging. The analysis of the surface topography formation under a wider range of process parameters (power variation, focus position, different materials), more complex structures, and real-time information about the LRM process delivered by a thermographic camera will be also considered in the future as a stepping stone towards the development of a real-time control system as well as optimization of the SSS-LRM process.

Acknowledgment

The work presented in this study is the result of the collaboration between Western University (London, Ontario, Canada) and National Research Council of Canada.

References

[1] F. D. Ince and T. Ozel, “Laser surface texturing of materials for surface functionalization: A holistic review,” Surface & Coatings Technology, 2025, 498, paper 131818, 26 pp.

[2] T. D. Bennett, D. J. Krajnovich, and L. Li, "Thermophysical modeling of bump formation during CO_2 laser texturing of silicate glasses," Journal of Applied Physics, 1999, 85(1), pp. 153-159.

[3] A. L. Buxton and B. G. I. Dance, “Surfi-Sculpt™ - Revolutionary surface processing with an electron beam,” Proc. of the 4th Int’l Surface Engineering Congress, 2005, pp. 107-110.

[4] X. Wang, J. Ahn, Q. Bai, W. Lu, and J. Lin, “Effect of forming parameters on electron beam Surfi-Sculpt protrusion for Ti-6Al-4V,” Materials and Design, 2015, 76, pp. 202–206.

[5] A. Temmler, E. Willenborg, and K. Wissenbach, "Design surfaces by laser remelting," Physics Procedia, 2011, 12, pp. 419-430.

[6] A. Temmler, M. A. Walochnik, E. Willenborg, and K. Wissenbach, "Surface structuring by remelting of titanium alloy Ti6Al4V," J of Laser Applications, 2015, 27(S2), paper S29103, 8 p.

[7] F. E. Pfefferkorn, J. D. Morrow, “Controlling surface topography using pulsed laser micro structuring,” CIRP Annals, 2017, 66, pp. 241–244.

[8] E. V. Bordatchev, M. Küpper, S. J. Cvijanovic, E. Willenborg, N. Milliken, A. Temmler, O. R. Tutunea-Fatan, “Edge-lit sine-shape wedged light guides: Design, optical simulation, laser-remelting-based precision fabrication, and optical performance evaluation,” Precision Engineering, 2020, 66, pp. 333–346.

[9] O. Oreshkin, M. Küpper, A. Temmler, and E. Willenborg, "Active reduction of waviness through processing with modulated laser power," Journal of Laser Applications, 2015, 27(2), paper 022004, .

[10] L. Kreinest, B. Schober, E. Willenborg, and J. Stollenwerk, "Investigation of asymmetry reduction for surface structuring and destructuring by laser remelting," Heliyon, 2024, 10(2), paper e24067, 14 p.

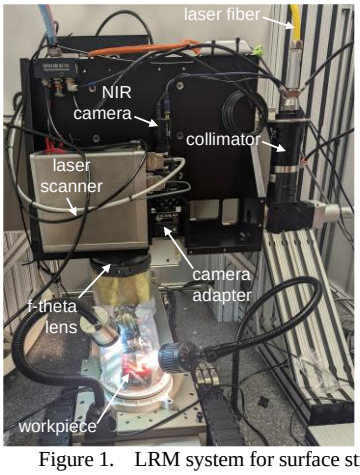

Figure 1. LRM system for surface structuring and surface texturing.

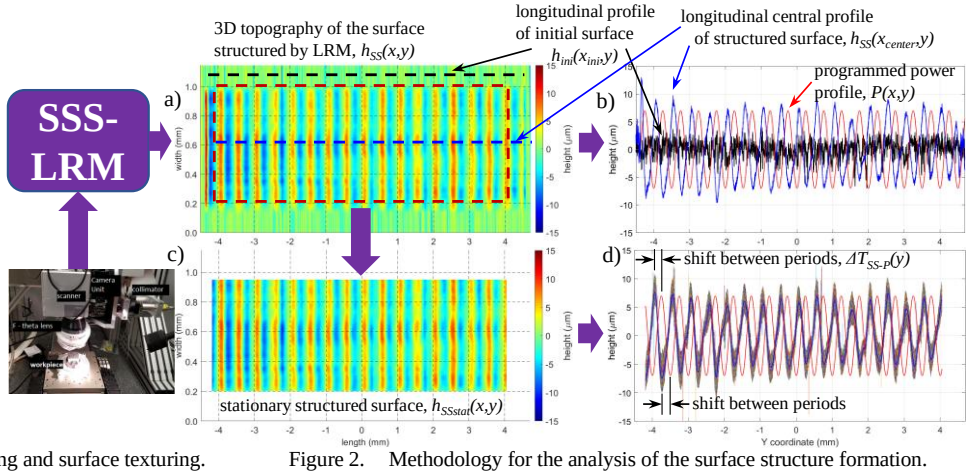

Figure 2. Methodology for the analysis of the surface structure formation.

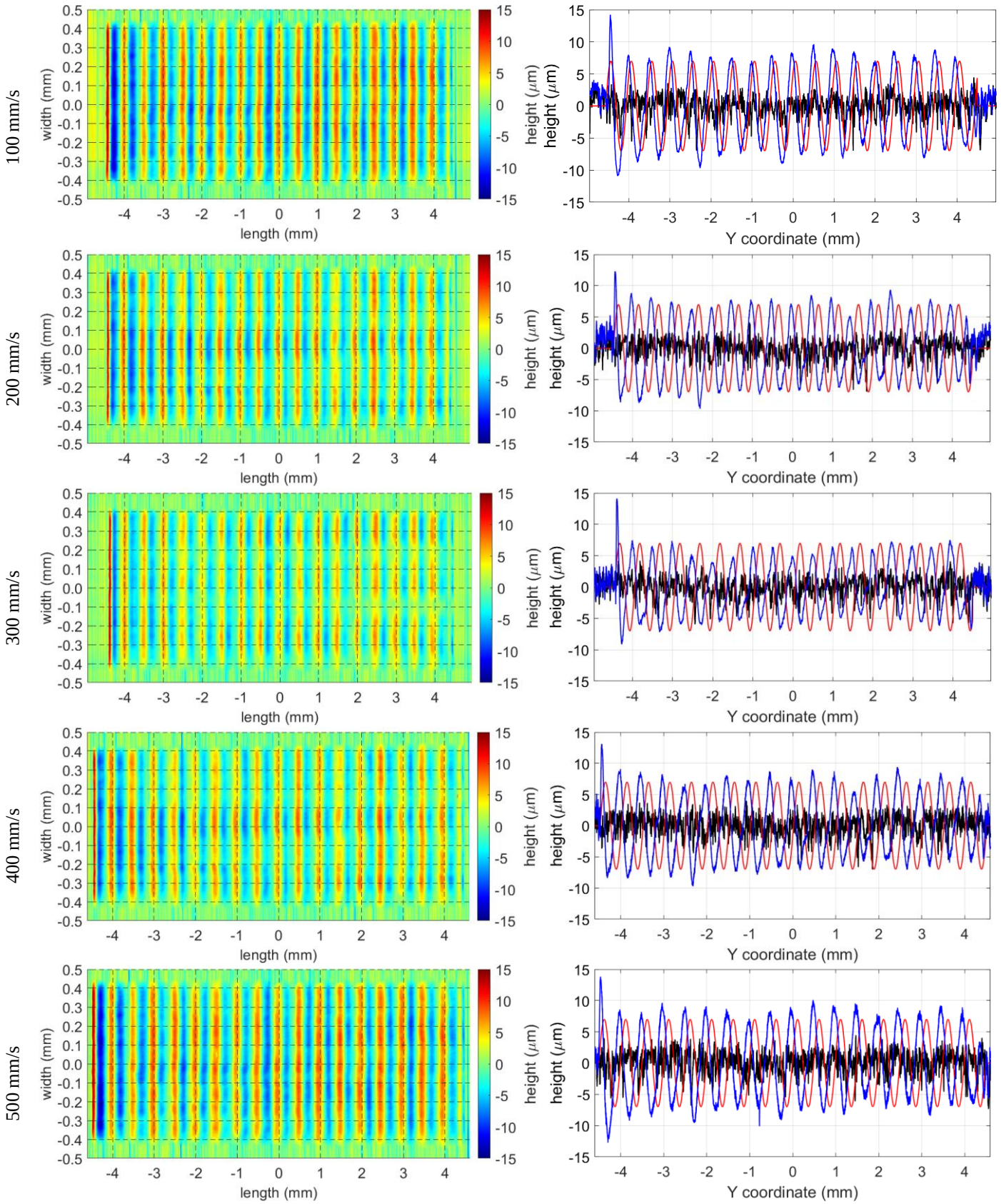

Figure 3. Surface topographies (left column) and longitudinal profiles (right column): initial (black), desired (red), and middle actual (blue).

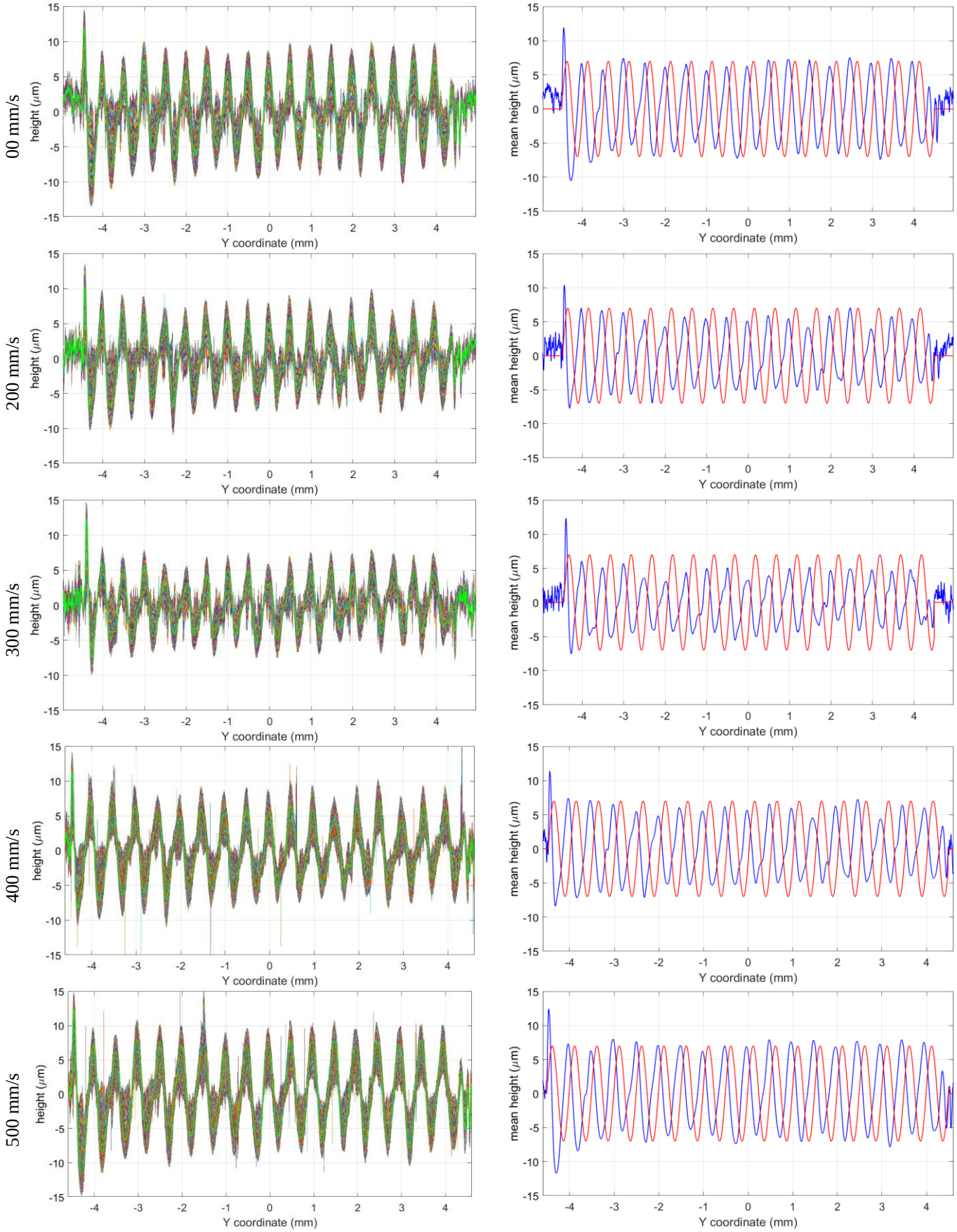

Figure 4. Longitudinal profiles: all actual and their averaged (left column, green) and desired and averaged actual (right column, red, blue)